Experimental Investigation of Key Structural Parameters for Structural Design of 3D-Printed Concrete

Jørgensen, Henrik Brøner; Hansen, Steen Nedergaard Lillebro; Jespersen, Esra Tøste Lomholdt; Florenzano, Daniele; Naboni, Roberto

Published in:
ReConStruct

Publication date:
2024

Document version:
Final published version

Citation for pulished version (APA):
Jørgensen, H. B., Hansen, S. N. L., Jespersen, E. T. L., Florenzano, D., & Naboni, R. (2024). Experimental Investigation of Key Structural Parameters for Structural Design of 3D-Printed Concrete. In R. S. Henry, & A. Palermo (Eds.), *ReConStruct: Resilient Concrete Structures - Proceedings of the 20th fib Symposium, 2024* (pp. 2945-2956). fib.

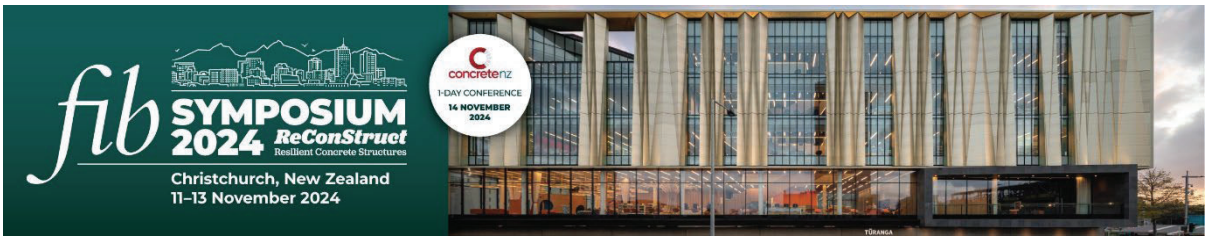

Experimental Investigation of Key Structural Parameters for Structural Design of 3D-Printed Concrete

Henrik B. Jørgensen[1,*], Steen N. L. Hansen[1], Esra Jespersen[1,2], Daniele Florenzano[3] and Roberto Naboni[3]

[1] SDU Structures, Department of Technology and Innovation, University of Southern Denmark, Odense, Denmark
[2] Rambøll A/S, Copenhagen, Denmark
[2] SDU CREATE, Department of Technology and Innovation, University of Southern Denmark, Odense, Denmark
*hebj@iti.sdu.dk

Abstract. The use of robots to produce 3D-printed concrete structures is developing rapidly. The technology offers promising potential to change the way we design and optimise concrete structures. This has already been shown by numerous publications in academia and showcased in the industry.
When developing new design expressions for 3D-printed concrete structures or adopting well-known models for cast concrete structures from the literature, it is important to be able to test the basic material characteristics. First, when the models are developed in academia. Secondly, to be able to test the material characteristics of printed material onsite.
The design models for cast concrete are typically based on the compressive strength of concrete and implicitly include the tensile strength. However, we do not have the same evidence for the relation between compressive and tensile strength for printed concrete. In addition, it is expected that the relation is not the same in all directions, because of the layered printing process.
This paper proposes a testing methodology for testing the tensile strength of robotically printed concrete. Furthermore, the paper presents experimental and statistical evidence for the anisotropic compressive and tensile strength of printed concrete.

Keywords: 3D Concrete Printing, Testing methodology, Experimental investigation, Anisotropy, Compressive strength, Tensile strength

1 Introduction

For the last decade, research and development within 3D-printed concrete structures have largely been focused on the development of material composition, the automation of the print process and the development of dedicated equipment for industrial robots. While studies on printed structural elements have been conducted by several, e.g. [1-3], there is still a lack of knowledge on the design and load-bearing capacity calculation of 3D-printed concrete structures. Currently, industry projects are based on "design by testing", which strongly limits the adoption of this construction method.

The determination of the bearing capacity of conventionally cast concrete structures is based on the compressive strength of the concrete, which is determined by testing cast cylinders. According to the codes and standards, the concrete tensile strength can be calculated on the basis of the compressive strength, and the strength is assumed to be equal across a structure, and for all directions [4-6]. In structures made with 3D Concrete Printing (3DCP), these assumptions are not valid. As shown in the

literature the layering of the concrete often gives an anisotropic compressive strength [7]. Furthermore, the calculation of the tensile strength cannot be calculated using the model from cast concrete, as the tensile strength varies in the different directions.

To be able to develop reliable mechanical models and to design 3D-printed concrete structures with mechanical models, a better understanding of the material characteristics and the structural behaviour is required. This includes understanding the anisotropic material behaviour in tension and compression and the relation in between. Furthermore, standardised methods for testing the material characteristics are needed. Standardisation is important to be able to use the same methods for producing experimental evidence in the laboratory as will be used for material characteristics in practice.

This paper provides experimental evidence on the material characteristics of 3D-printed concrete. This is achieved by comparing samples obtained from 3D-printed, cast, and mould-cast specimens. From these samples, the concrete compressive and tensile strength are found for the three main directions.

2 Experimental programme

2.1 Specimens

The experimental programme tested 63 specimens in compression and 58 specimens in tension. The specimens were produced as a mix of specimens extracted from printed and cast blocks and specimens cast in different kinds of moulds for material testing. Fig. 1 shows the general design of the printed blocks and a randomised placement of the specimens which were extracted from the blocks. The printing campaign consisted of two printing sessions, conducted in comparable environmental conditions. The first session produced 7 printed blocks with dimensions 1150x550x230mm, 2 cast blocks of the same dimensions, 14 mould-cast cylinders, and 8 mould-cast Wedge Splitting Test (WST) specimens. The second session produced 3 printed blocks of dimensions 750x440x230mm, one cast block of dimension 405x275x225mm, and 6 mould-cast cylinders. The designed filament geometry of the printed blocks was approximately 35x10mm.

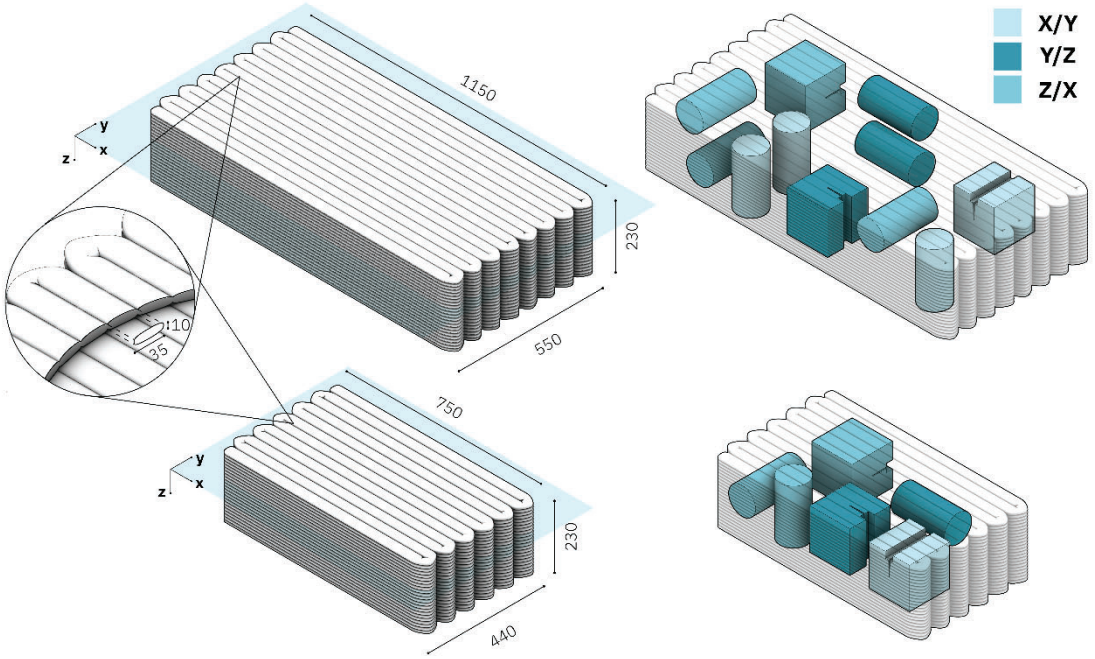

Fig. 1. Design properties and dimensions of printed blocks with zoom on filament proportions (left) and example of placement of material samples within the printed block for extraction, with different orientations with respect to filament principal direction (right).

The position for the extraction of the printed specimens has been devised to maximise the variability of the element composition by spreading the distribution of the printed specimens within each block. The main orientations of the specimens permit the testing of the compressive and tensile capacity of printed specimens in 3 different orientations with respect to the main printing direction, as shown in Fig. 1. Where relevant, the exact coring position was planned to match the need for testing the specimen strength at the position of the layer interface.

Fig. 2 shows an overview of all types of specimens. The extracted specimens are shown with the specimen layer orientation, highlighting the printing plane in the X, Y and Z configurations. Similarly, specimens in the same directions were extracted from the cast blocks. The specimen size is identical for extracted specimens and mould-cast specimens.

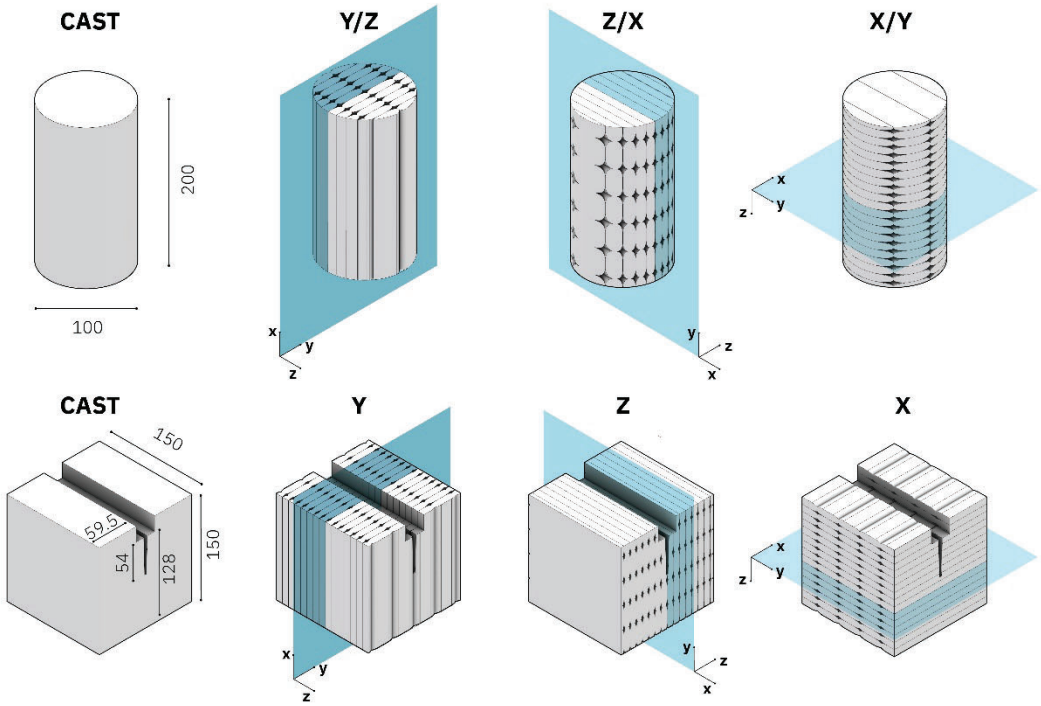

Fig. 2. Overview of specimens; Mould-cast specimens (left) and extracted specimens from the printed blocks with visualisation of printing plane (right). The notation above specimens shows the direction in which the specimen can test tensile strength.

2.2 Material properties

The specimens were printed using an adapted formulation from Weber Elementfugemørtel 35, a commercial bedding mortar with thixotropic behaviour, typically utilised for joints within prefabricated concrete elements. The printing mortar is formulate with 50-58% of aggregates (0-2mm), 38-44% Portland cement and 8-12% additives. See Table 1 for pertinent material data. The dry mixture has a density of 2.1 kg/l, and its preparation involved continuously mixing the dry premix with 19% water content in the pump.

Table 1. Concrete mix for printing

	Mixture
Material type	Elementfugemørtel 35 MPa
Environmental class	Aggressive
Exposure class	X0/XC4/XS3/XD2/XF4/XA1
Cement type	Portland Cement CEM I 52.5 N (MS) (LA)
Aggregate type	Quartz sand
Aggregate size	0-2 mm

2.3 3D concrete printing method

The 3D printed blocks were fabricated at the CREATE Lab's robotic facility within the University of Southern Denmark (SDU). The setup employed a six-axis ABB IRB 6650S robot with a maximum reach of 3.3 m, and a Vergumat P06 continuous mixing cavity pump, with a capacity of 56 l/m. The extrusion head, featuring a circular nozzle with a diameter of 25 mm, incorporated an AKO VMC20 pinch valve, to control the initiation and termination of the extrusion process via programmed digital outputs, which are synchronised with the control of the mixing pump [8].

In 3DCP, the toolpath generation process involves translating a 3D digital model into machine-readable code to guide layered extrusion. To achieve this, a framework was developed to transform the input geometry into polylines at defined distances, determining the height of printed layers [9].

The specific cross-sectional shape of the filament is influenced by parameters such as movement speed, layer height, and nozzle orientation, with the nozzle diameter and material mix being constant factors. These variables also determine the layer width and, consequently, the sectional shape of the layer, which impacts surface contact [10]. Accordingly, the specimens were generated through continuous polylines which were then converted into a list of planes, to which a constant speed of 200mm/s has been associated. The identified plane lists and speed values were translated into motion trajectories for the industrial robot through the utilisation of the Grasshopper plugin Robots. To facilitate the transition between one layer and the other, selected planes have been assigned specific digital outputs to switch on and off the pump and control the extrusion from the head.

2.4 Specimen extraction from blocks

The extraction of the specimens are briefly described. A more detailed description of the experimental programme and the results can be found in [11]. All printed and cast blocks were cured for at least three weeks before the extraction. The blocks were marked for measurements in each of the cardinal directions before being cut into smaller blocks. The cylinders for compressive- and Brazilian split testing were extracted by coring from the blocks, shortening them using a hacksaw, and grinding them to their desired length of 200 mm using a pillar drill mounted with a cup grinding disc.

Fig. 3 shows the WST specimens being extracted from the blocks. Firstly, by sawing the wedge notch and groove into the block piece. Secondly, material was removed from around the specimen with a concrete saw. Finally, the rough shape of the specimen was ground to the desired dimensions using an angle grinder with a diamond grinding disc.

The WST specimens were ground on all sides that would have contact with the testing components. This meant that the top, bottom, front and back of the specimen were ground.

3 Testing methodology

3.1 Compressive testing methodology

The compressive strength was tested using a standard hydraulic compression machine. The tests were performed using a displacement-controlled test scheme, set to a linear strain increase, which allows for visualisation of the compression softening curve. The test follows the European standard DS/EN 12390-3 for compressive tests on concrete [12] and is tested with a displacement-controlled speed of 0.007 mm/s. It should be noted that while DS/EN 12390-3 prescribes a loading rate between 0.4-0.8 MPa/s, the loading rate in this study was approx. 0.3 MPa/s.

3.2 Tensile testing methodology

The experimental programme was established with two different methods for testing the tensile strength. Fig. 4 shows a schematic drawing of the tensile testing of the two types of specimens. Here, it can be seen that both tests are focused on testing the tensile strength in different directions and include testing the tensile strength between the printed layers. Fig. 5 shows the failure mode of the two different types of tensile tests. It can be observed that the crack development and thereby the tested tensile strength was different, as further detailed in the next section.

Fig. 3. Method for cutting blocks and notches for WST specimens, notches cut into specimens, and the specimen placement inside the blocks once extracted.

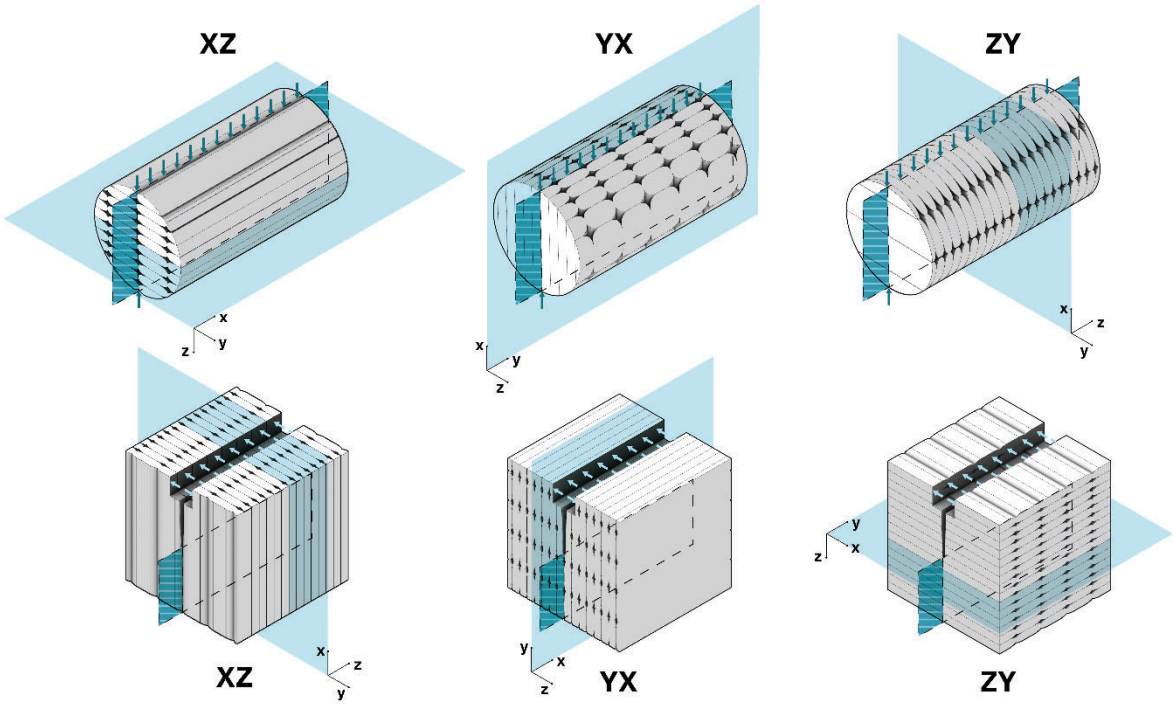

Fig. 4. Visualization of acting forces and rupture planes with respect to printing plane for all types of specimens in both Brazilian split tests and Wedge splitting tests. The notation above and below the specimens show the plane in which the tensile stresses occur, i.e XZ = y-direction tensile stress, YX = z-direction tensile stress and ZY = x-direction tensile stress.

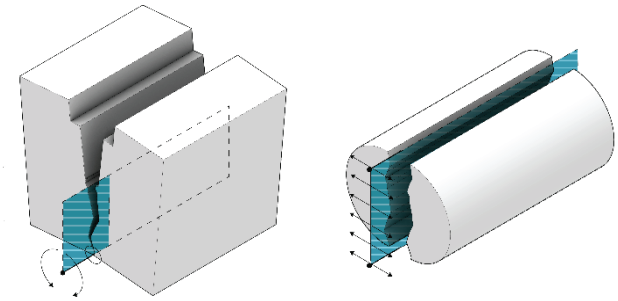

Fig. 5. Failure modes of the two types of tensile tests. On the left, the failure mode of the Wedge Splitting Test involves the specimen being split in two parts with the parts rotating around a shared point at the bottom of the specimen. On the right, the failure mode of the Brazilian split test involves the two parts of the specimen moving translatoric away from each other.

Brazilian split tests. The Brazilian split test is an indirect tensile testing method performed using a hydraulic machine, which can be seen in Fig. 6. The test was performed in accordance with DS/EN 12390-6 [13]. The setup included two metal plates with a convex side. In between the specimen and the metal plates, high-density fibreboards were placed to soften the contact from inconsistencies that would otherwise cause stress concentrations. When a vertical force, P, is diametrically applied in a line spanning the length of the cylinder specimen, a stress distribution perpendicular to the loading plane forms. The tensile strength is then obtained with the following expression:

$$f_{ct} = \frac{2 \cdot P}{L \cdot \pi \cdot D} \tag{1}$$

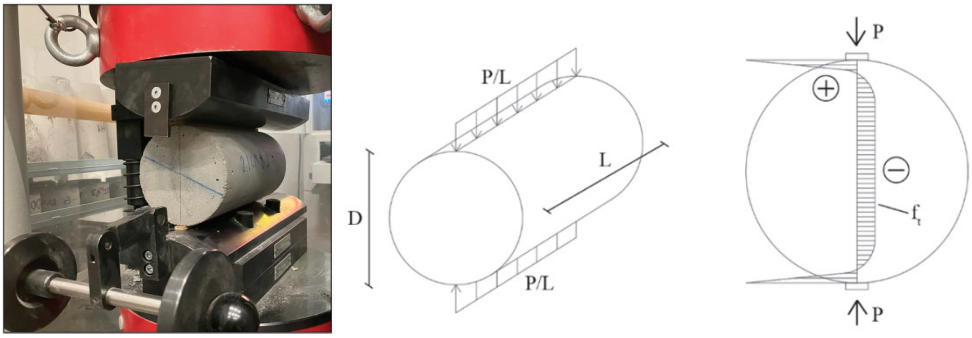

Fig. 6. Test setup BST, loading application and stress distribution inside the specimen. (+) and (-) denotes compressive and tensile stresses, respectively.

Wedge splitting tests. The WST was originally developed by Linsbauer and Tschegg [14] and later further developed by Brühwiler and Wittmann [15] to determine the fracture energy of a material. This was done by implementing the hinge model proposed by Ulfkjær and Olesen [16] using the fictitious crack model by Hillerborg [17] initially used for plain concrete. Using the WST and cracked hinge model, a method of parameter estimation developed by Østergaard [18] was applied to extract the stress-crack opening relationship.

The WST is shown in Fig. 7. The force is applied by a steel wedge, through contact with roller bearings, which creates a moment and consequently a stress distribution in the specimen area below the notch. A clip-gauge extensometer, placed in the wedge specimen groove, measures the crack mouth opening displacement, CMOD, which paired with the vertical force applied on the specimen provides an F_v-CMOD curve for analysis. The tests were displacement-controlled, measured from the vertical displacement of the machine crosshead, and were conducted with a test speed of 0.4 mm/min from start until 70% of the maximum load from where it was changed to 0.1 mm/min.

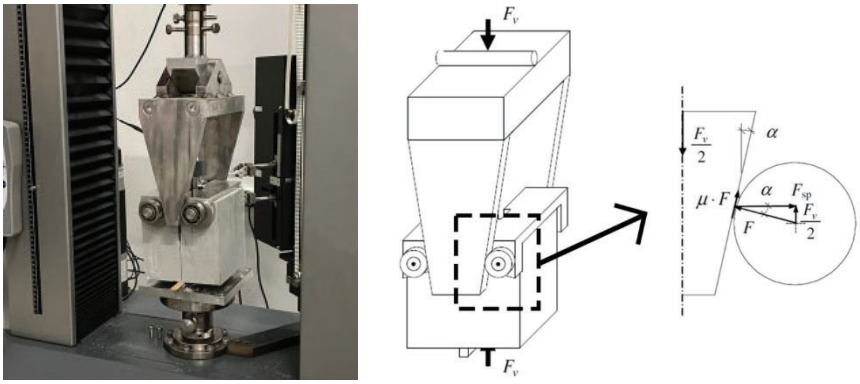

Fig. 7. The test setup and free body diagram of the acting forces in the test. Figure recreated from [18,19].

The horizontal splitting force, F_{sp}, can be calculated based on the free-body diagram:

$$F_{sp} = \frac{1}{2} F_v \cot(\alpha) \tag{2}$$

F_v-CMOD curves are extracted, simulated values of F_{sp} and CMOD can be computed through an iterative process and the constitutive parameters of the bilinear softening curves can be found through inverse analysis. It is assumed in the cracked hinge model that cracks only influence stress- and strain fields locally. The idea is that the material close to the crack acts as independent spring elements, formed by incremental strips connecting the rotating bodies of the hinge model [16]. The hinge model allows cracked geometry to interact with the uncracked part of the specimen. The bilinear curve is visualised in Fig. 8.

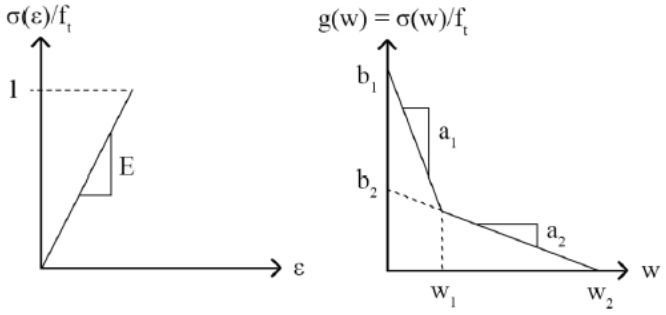

Fig. 8. The elastic stress-strain curve followed by the bilinear stress-crack opening relationship. Figure recreated from [16,19].

When fitting the computed F_{sp}-CMOD curve to the observed/measured data, two nonlinear equations are used to find the actual splitting force. These two equations act as the restraints on the load, and are as follows [18]:

$$\mu_{ext}(F_{sp}) - \mu_{int}^{j}(\theta, F_{sp}) = 0 \tag{3}$$

$$CMOD^{obs} - CMOD(F_{sp}, \theta) \tag{4}$$

It has been shown in the literature that using a tensile softening curve (bilinear curve of the stress-crack opening relationship) yields accurate predictions of the tensile strength of concrete [18].

4 Results

4.1 Compressive strength

Table 2 shows the mean value of the compressive strength of the specimens tested in the x- y- and z-directions and the strength of the specimens drilled from the cast blocks (cut cast) and the mould cast specimens. Figure 10 shows a boxplot of the same data. These results are similar to previously published results [7], with the x-direction having a larger strength than the other directions and a lower strength than the mould cast cylinder. However, this study also shows that the strength of a core extracted from a cast block has a similar strength as a core extracted from the printed blocks.

Table 2. Mean values, standard deviation and sample size of the CCT specimens

	Mean value [MPa]	Std Dev [MPa]	Sample size [No.]
X-direction	45.5	4.4	19
Y-direction	35.0	7.5	14
Z-direction	36.7	2.8	18
Cut cast	41.0	5.7	6
Mould cast	54.5	3.7	6

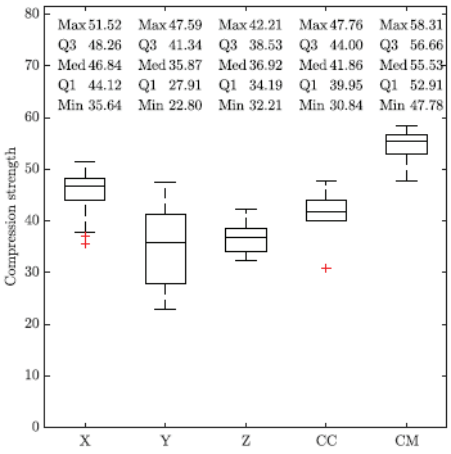

Fig. 10. Boxplot of tested compressive strengths in x- y- and z-directions.

4.2 Tensile strength

Tables 3 and 4 show the mean value of the tensile strength of the Brazilian split specimens and WST specimens, respectively. Fig. 11 shows boxplots of the same data. Here, it can be observed that the tensile strength in the YX-plane (Z-direction, i.e. the tensile strength between the layers) is significantly lower than the strength in the other directions when tested as a Brazilian split test. On the other hand, the tensile strength seems to be similar in all directions when tested as a WST specimen. It is noted that the tensile strength of specimens extracted from printed blocks is similar to those extracted from the cast blocks. In contrast, the mould cast specimens generally show a significantly higher strength than the extracted specimens.

Table 3. Mean values, standard deviation and sample size of the BST specimens

	Mean value [MPa]	Std Dev [MPa]	Sample size [No.]
ZY-plane (X-direction)	2.7	0.30	16
XZ-plane (Y-direction)	2.6	0.37	13
YX-plane (Z-direction)	2.0	0.38	14
Cut cast	2.7	0.21	8
Mould cast	3.3	0.22	7

Table 4. Mean values, standard deviation and sample size of the WST specimens

	Mean value [MPa]	Std Dev [MPa]	Sample size [No.]
ZY-plane (X-direction)	1.3	0.32	7
XZ-plane (Y-direction)	1.2	0.14	7
YX-plane (Z-direction)	1.1	0.20	6
Cut cast	1.2	0.14	7
Mould cast	1.4	0.22	7

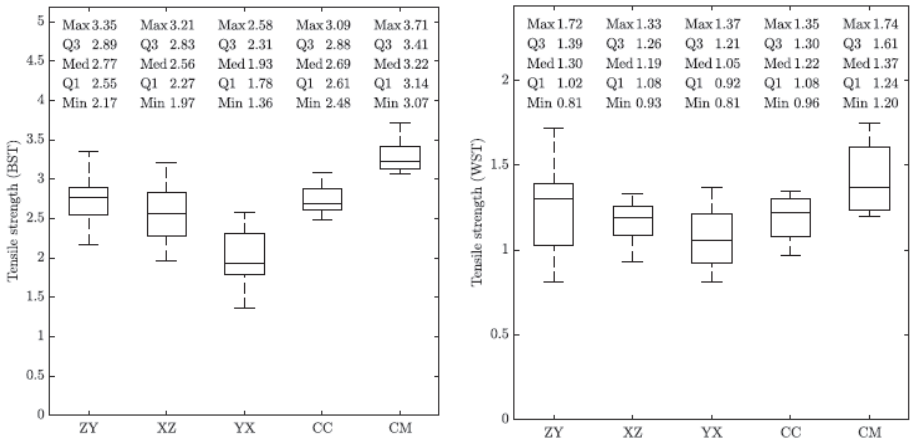

Fig. 11. Boxplot of; tensile strengths of Brazilian split specimens **(left)** and tensile strengths of WST specimens **(right)**.

5 Conclusions

This paper presents an experimental programme comprising 63 specimens in compression and 58 specimens in tension. The experimental programme compares the compressive and tensile strength of cast concrete and 3D Printed Concrete. The main conclusions from the study are:

- The compressive strength in the X-direction (the main printing direction) is significantly larger than the strength in the other directions.
- The compressive strength of a cylinder extracted from a cast concrete block is shown to have a slightly lower strength than the X-direction of the printed block and a slightly larger strength than the other directions.
- The compressive strength of a mould cast cylinder is significantly larger than the strength of all extracted cores.
- When testing the tensile strength as a so-called Brazilian split specimen, the tensile strength in the Z-direction is significantly lower than in the other directions.
- When testing the tensile strength as a Wedge split test specimen, the tensile strength is approximately the same in all directions.
- The tensile strength of the specimens extracted from the cast blocks is generally the same as those extracted from a 3D Printed block.
- The tensile strength of mould cast cylinders is significantly larger than the extracted specimens.

Acknowledgements

This experimental project was carried out at the University of Southern Denmark. The fabrication was conducted at SDU CREATE Lab and structural testing performed at SDU Structures Lab. The authors thank industrial partners Hyperion Robotics and Weber Saint Gobain Denmark (printing mortar). This work has been conducted as part of the project "3D Printed Concrete and standardised testing methods" funded by We Build Denmark and the Danish Ministry of Higher Education and Science.

References

1. Gislason, S, Bruhn, S, Breseghello, L, Sen, B, Liu, G, & Naboni, R (2022). Porous 3D printed concrete beams show an environmental promise: a cradle-to-grave comparative life cycle assessment. Clean Technologies and Environmental Policy, 24(8), 2639-2654. https://doi.org/10.1007/s10098-022-02343-9
2. Gosselin C, Duballet R, Roux P, Gaudillière N, Dirrenberger J, Morel P (2016) 'Large-scale 3D printing of ultra-high-performance concrete – a new processing route for architects and builders', Materials & Design, vol. 100, pp. 102–109, Jun. 2016, doi: 10.1016/j.matdes.2016.03.097.
3. Gebhard L, Mata-Falcón J, Anton A, Dillenburger B, Kaufmann W (2021) 'Structural behaviour of 3D printed concrete beams with various reinforcement strategies', Engineering Structures, vol. 240, p. 112380, Aug. 2021, doi: 10.1016/j.engstruct.2021.112380.
4. DS/EN:1992-1-1 (2008). Eurocode 2: Design of concrete structures - Part 1-1: General rules and rules for buildings
5. fib Model Code 2010 (2013). Fédération Internationale du Béton, fib Model Code for concrete structures 2010. Ernst & Sohn
6. ACI 318-19 (2019). Building code requirements for structural concrete: Commentary on building code requirements for structural concrete. American Concrete Institute
7. Jørgensen, HB, Douglas, PJ, Naboni, R (2021). Experimental Study on the Anisotropic Behaviour and Strength of 3D Printed Concrete. I E. Julio, J. Valenca, & A. S. Louro (red.), Concrete Structures: New Trends for Eco-Efficiency and Performance, Proceedings for the 2021 fib Symposium, Portugal, pp. 739-748. International Federation for Structural Concrete.
8. Breseghello L, Hajikarimian H, Jørgensen HB, and Naboni R (2023) '3DLightBeam+. Design, simulation, and testing of carbon-efficient reinforced 3D concrete printed beams', Engineering Structures, vol. 292, p. 116511, Oct. 2023, doi: 10.1016/j.engstruct.2023.116511.
9. Breseghello L, Naboni R (2022) 'Adaptive Toolpath: Enhanced Design and Process Control for Robotic 3DCP', in Computer-Aided Architectural Design. Design Imperatives: The Future is Now, vol. 1465, D. Gerber, E. Pantazis, B. Bogosian, A. Nahmad, and C. Miltiadis, Eds., in Communications in Computer and Information Science, vol. 1465, Singapore: Springer Singapore, 2022, pp. 301–316. doi: 10.1007/978-981-19-1280-1_19.
10. Breseghello L, Naboni R (2022) 'Toolpath-based design for 3D concrete printing of carbon-efficient architectural structures', Additive Manufacturing, vol. 56, p. 102872, Aug. 2022, doi: 10.1016/j.addma.2022.102872
11. Hansen SNL, Jespersen ETL (2024) Experimental investigation of the load-bearing capacity of 3D Printed Concrete Structures - A study of the influence of the anisotropic properties of printed concrete, Master's Thesis, University of Southern Denmark, Odense, Denmark
12. DS/EN-12390-3 (2019). Testing hardened concrete – Part 3: Compressive strength of test specimens. Göteborg Plads 1, Dk 2150 Nordhavn
13. DS/EN-12390-6 (2012). Testing hardened concrete - Part 6: Tensile splitting strength of test specimens. Kollegievej 6, Dk 2920 Carlottenlund.
14. Linsbauer H, Tschegg E (1986) Determination of fracture energy determination of concrete with cube-shaped specimens, Article, Zement und Beton, 31. Jarhgang, Heft 1, Insitut für Konstruktiven Wasserbau, Institut für Angewandte Physik, 1040 Wien, Karlsplatz 13
15. Brühwiler E, Wittmann FH (1990). THE WEDGE SPLITTING TEST, A NEW METHOD OF PERFORMING STABLE FRACTURE MECHANICS TESTS, Engineering Fracture Mechanics Vol. 35, No. 1/2/3, pp. 117-125, Swiss Federal Institute of Technology, Laboratory for Building Materials, Lausanne, Switzerland
16. Olesen, JF (2001). "FICTITIOUS CRACK PROPAGATION IN FIBER-REINFORCED CONCRETE BEAMS", Journal of Engineering Mechanics, pp. 272-280, March 2001

17. Petterson P, Hillerborg A (1981). CRACK GROWTH AND DEVELOPMENT OF FRACTURE ZONES INPLAIN CONCRETE AND SIMILAR MATERIALS, PhD thesis, Report TVBM Vol. 1006, Div. of Building Materials, Lund Institute of Technology
18. Østergaard L (2003). "Early Age Fracture Mechanics and Cracking of Concrete". PhD thesis, Technical University of Denmark. BYG-Rapport No. R-070.
19. Ingemar L, Olesen JF, Flansbjer M (2004). Application of WST-method for fracture testing of fibre-reinforced concrete Application of WST-method for fracture testing of fibre-reinforced cement based composites. ISSN 1651-9035, Report 04:13, Archive no. 35, Department of Structural Engineering and Mechanics, Concrete Structures, Chalmers University of Technology